1,2- vs 1,4-Regioselectivity of Lithiated Phenylacetonitrile toward α,β-Unsaturated Carbonyl Compounds. 1. Monomer−Dimer Equilibrium of Lithiated Phenylacetonitrile Ion Pairs in Solution and Structure Determination of the Species by Spectroscopic Methods and ab Initio Calculations. Evidence of a Lithium Bridged Monomeric Ion Pair

Tekla Strzalko, Jacqueline Seyden-Penne, and Lya Wartski*

Institut de Chimie Moléculaire d'Orsay, URA CNRS 478, 91405 ORSAY, France

Jacques Corset,* Martine Castella-Ventura, and Françoise Froment

LASIR, CNRS, UPR 2631, B.P. 28, 94320 Thiais, France

Received July 30, 1996 (Revised Manuscript Received August 6, 1997)

New contributions from near-infrared FT-Raman and IR spectroscopies to the structure of $[PhCHCNLi]_n$ (**1**) in solution evidence that only two species, a monomeric ion pair **2** and a dimeric one **4**, are in equilibrium in media of low dielectric constants such as THF, THF−toluene, or THF−hexane solvent mixtures. The equilibrium position is directly related to the dielectric constant of the medium, and the integrated molar absorption coefficient of each species is determined. The THF-solvated dimer **4** has a structure very close to that of the TMEDA-solvated dimer **3** in the solid state, the two phenyl groups being in an anti arrangement and the nitrogen atom of the $C_{1'}N$ bond interacting with the two lithium cations. The comparison of ab initio calculations with IR and ^{13}C NMR data of the lithiated monomer **2** shows that its structure is a bridged one in which the lithium cation interacts mainly with the $C_{2'}$ carbon in the α position to the nitrile group, with the ipso $C_{3'}$ carbon of the phenyl group, and to a lesser extent with the $C_{4'}$ carbon of the phenyl group. Low-temperature ^{13}C NMR indicates a lower rotational barrier of the phenyl group for the monomeric lithiated ion pair **2** than for the free anion.

Introduction

It is well-known that metalated benzylic nitriles are powerful synthons in organic synthesis.[1] A better knowledge of their structure is thus an essential goal in the understanding of their reactivity.

In a previous work, we carried out a detailed IR and ^{13}C NMR structural study of lithiated phenylacetonitrile $[PhCHCNLi]_n$ (**1**) in solution.[2,3] We have shown that solvent-separated ion pairs and free anions were present in THF−HMPA and DMSO at a concentration $C = 0.25$ M. In THF at $C = 0.25$ M, highly predominating monomeric tight ion pairs **2** were in equilibrium with aggregates, while at $C = 0.025$ M only the former species were characterized. The aggregated species increased with the amount of hexane in THF solutions ($C = 0.25$ M).

Recently, some papers appeared on the structure of metalated phenylacetonitrile in solution. Solvent separated ion pairs were studied by ^{13}C NMR,[4] IR, and ab initio force field calculations.[5] The site of metalation and the degree of aggregation of **1** in different solvent mixtures were examined by ^{13}C and $^{6}Li/^{15}N$ NMR.[6]

We previously reported[2,3] that in THF, next to the $\nu(C\equiv N)$ band characteristic of the monomeric species **2**, seen by IR at 2090 cm^{-1}, there are two other $\nu(C\equiv N)$ bands at 2072 and 2058 cm^{-1}, which were ascribed to two different aggregated species, as their intensities increased in THF−hexane mixtures. The behavior of the band at 2072 cm^{-1} was apparently different from that of the band at 2058 cm^{-1}. To get a better understanding of the aggregation state of **1**, we report herein the IR and near-infrared Fourier transform Raman study of **1** in THF and in different THF−hexane and THF−toluene solvent mixtures at a fixed concentration $C = 0.25$ M and of the crystalline dimeric TMEDA-solvated species described by Boche[7] $[(PhCHCNLi{\cdot}TMEDA)_2{\cdot}C_6H_6]$ (**3**) that we have prepared. The use of NIR−FT Raman allowed us to obtain Raman spectra of organic solutions that could not be observed previously due to their fluorescence when excited in the visible region.

A recent theoretical study of dimeric species **3** by PM3 and MNDO calculations[8] prompted us to publish our ab initio calculations of the monomeric species **2**, as the location of the Li cation in **2** is still a matter of controversy. We have also compared our calculations to

(1) Arseniyadis, S.; Kyler, K. S.; Watt, D. S. *Org. React.* **1984**, *31*, 1−354.
(2) Croisat, D.; Seyden-Penne, J.; Strzalko, T.; Wartski, L.; Corset, J.; Froment, F. *J. Org. Chem.* **1992**, *57*, 6435.
(3) Strzalko, T.; Seyden-Penne, J.; Wartski, L.; Froment, F.; Corset, J. *Tetrahedron Lett.* **1994**, *35*, 3935.
(4) Abbotto, A.; Bradamante, S.; Pagani, G. A. *J. Org. Chem.* **1993**, *58*, 449.
(5) Binev, I. G.; Tsenov, J. A.; Velcheva, E. A.; Juchnovski, I. N. *J. Mol. Struct.* **1995**, *344*, 205.
(6) Carlier, P. R.; Lucht, B. L.; Collum, D. B. *J. Am. Chem. Soc.* **1994**, *116*, 11602.
(7) (a) Boche, G.; Marsh, M.; Harms, K. *Angew. Chem., Int. Ed. Engl.* **1986**, *25*, 373. (b) Boche, G. *Angew. Chem., Int. Ed. Engl.* **1989**, *28*, 277. (c) We are grateful to Professor Boche, who sent us a copy of the IR spectrum and revised X-ray data of the dimeric species $[(PhCHCNLi{\cdot}TMEDA)_2{\cdot}C_6H_6]$ ($\beta = 99.43$ and $R = 0.088$). (d) Langlotz, I. Ph.D. Thesis, Universität Marburg, 1993.
(8) Koch, R.; Wiedel, B.; Anders, E. *J. Org. Chem.* **1996**, *61*, 2523.

S0022-3263(96)01449-1 CCC: $15.00
Published on Web 04/28/1998

those of Schleyer[9] on the lithiated monomeric anionic species derived from CH_3CN. These structural studies allow us in the accompanying paper[10] to examine the influence of the aggregation state of **1** in THF at different concentrations and at $C = 0.25$ M in THF−toluene and THF−hexane solvent mixtures on the 1,2- vs 1,4-regioselectivity toward some α,β-unsaturated carbonyl compounds.

Experimental Section

Sample Preparation of 1. Experimental conditions were described previously.[2] After addition of 1.2 equiv of base, 1 M LHMDS in THF, or 1.6 M *n*-BuLi in hexane (in the case of Figure 3) to $PhCH_2CN$ in THF at 20 °C ($C = 0.25$ M) under argon, the solution was stirred during 30 min. The IR, Raman, and ^{13}C NMR spectra do not show any evolution within 12 h.

IR Spectra. Infrared spectra were scanned using a Perkin-Elmer 983 spectrometer at 3 cm^{-1} resolution.[2] The CaF_2 cell thicknesses were 0.003 to 0.004 cm. In IR spectra, the absorbance of the ν(C≡N) mode of the carbanionic species is very strong and depends on the solvent and species concentrations so that the thinnest 0.003 cm cell used may in some cases be too thick to accurately measure the concentration of the species.

Raman Spectra. Raman spectra were collected with a Perkin-Elmer system 2000R NIR FT-Raman spectrometer equipped with a stabilized Nd:YAG laser emitting at a wavelength of 1064 nm. Samples were excited at 180° backscattering mode using maximum laser power output of 500−1000 mW depending on the nature of the solution. The spectra were recorded at 4 cm^{-1} resolution in the wavenumber range 3600−200 cm^{-1} by accumulating about 200 scans in order to obtain a good signal-to-noise ratio (in Raman spectra the ν(C≡N) intensity of the carbanionic species is very weak in contrast to IR spectra). Frequency values are accurate to better than ±1 cm^{-1}, and the spectra were observed to be free from fluorescence. Samples were analyzed in glass containers (1 × 1 × 3 cm, rubber septum capped, purged with argon). The FT-Raman spectrum of solvent was measured and subtracted from each carbanionic solution Raman spectrum with an appropriate subtraction factor to cancel the solvent contribution.

NMR Spectra. ^{13}C spectra were recorded on a Bruker AM 250 or 400 spectrometer as in ref 2, operating at, respectively, 62, 9 and 100, 62 MHz. A 5 mm coaxial tube filled with CD_2Cl_2 located inside the 10 mm tube was used for the ^2H external lock.

Calculation Methods. Ab initio calculations were performed at the Hartree−Fock[11] level using the 3-21+G* basis set, with the GAUSSIAN92[12] and GAUSSIAN94[13] programs. In the 3-21+G* basis set, polarization and diffuse functions were added on all non-hydrogen atoms. The addition of diffuse functions is generally required for a proper description of anions. Complete geometry optimizations without any constraint were performed by means of the analytical gradient technique contained in the programs.

The Hartree−Fock total energies of the different species were determined at the equilibrium geometries with the 3-21+G* basis set. It is also necessary to point out that our calculations were run on isolated entities and do not take solvent effects into account.

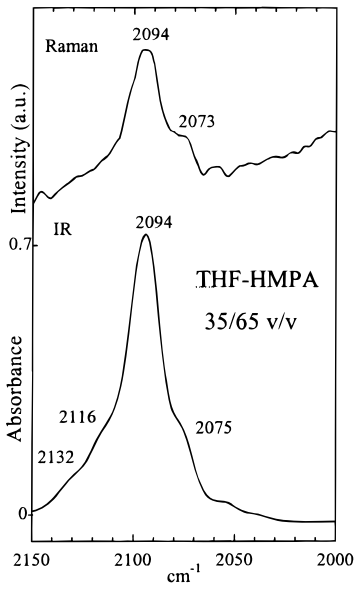

Figure 1. IR and Raman spectra in the ν(C≡N) region of **1** in THF−HMPA 35/65 v/v solvent mixture ($C = 0.25$ M).

Results and Discussion

(1) Monomer−Dimer Equilibrium Study by Near-Infrared FT-Raman and IR Spectroscopies. We first observed that the IR and Raman spectra of the solvent separated ion pair or free anion in the THF−HMPA 35/65 v/v solvent mixture (Figure 1) look very similar, with a main band at 2094 cm^{-1} and a shoulder at 2075 cm^{-1}, this latter band being assigned to a Fermi resonance between the ν(C≡N) mode and a combination of the carbanion skeleton modes.[14]

This assignment relies on the IR study[2] of the influence of the solvent, cryptand, cation, and carbanion concentration on the spectra evolution of **1**. Indeed, in DMSO or THF−HMPA mixtures at $C = 0.25$ M the main band appears at a wavenumber very close to that observed at 2096 cm^{-1} in THF for PhCHCNK in the presence of a stoichiometric amount of cryptand 222. In THF at $C = 0.25$ M, the ν(C≡N) band is observed at 2090 cm^{-1} for PhCHCNLi and at 2070 cm^{-1} for PhCHCNK. As the lithium cation has a larger polarization effect than the potassium one, the wavenumber is expected to be lower for PhCHCNLi than for PhCHCNK. This reverse effect will be explained later in regard to the structure of the ion pair **2**. The 2090 cm^{-1} band is also the only one that remains in THF when the concentration of PhCHCNLi decreases by a factor of 10. The assignment of the band at 2090 cm^{-1} to **2** is thus in agreement with Bauer and Seebach's cyroscopic determinations at similar concentration,[15] although the experiments have been carried out

(9) Kaneti, J.; Schleyer, P. v. R.; Clark, T.; Kos, A. J.; Spitznagel, G. W.; Andrade, J. G.; Moffat, J. B. *J. Am. Chem. Soc.* **1986**, *108*, 1481.
(10) Strzalko, T.; Seyden-Penne, J.; Wartski, L.; Corset, J.; Castella-Ventura, M.; Froment, F. *J. Org. Chem.* **1998**, *63*, 3295−3301.
(11) Roothan, C. C. *J. Rev. Mod. Phys.* **1951**, *23*, 69.
(12) Frisch, M. J.; Trucks, G. W.; Head-Gordon, M.; Gill, P. M.; Wong, M. W.; Foresman, J. B.; Johnson, B. G.; Schlegel, H. B.; Robb, M. A.; Replogle, E. S.; Gomperts, R.; Andres, J. L.; Rhaghavachari, K.; Binkley, J. S.; Gonzalez, C.; Martin, R. L.; Fox, D. J.; Defrees, D. J.; Baker, J.; Stewart, J. P.; Pople, J. A. *Gaussian 92*, Revision A, Gaussian, Inc., Pittsburgh, PA, 1992.
(13) Frisch, M. J.; Trucks, G. W.; Schlegel, H. B.; Gill, P. M. W.; Jonhson, B. G.; Robb, M. A.; Cheeseman, J. R.; Keith, T. A.; Petersson, G. A.; Montgomery, J. A.; Rhaghavachari, K.; Al-Laham, M. A.; Zakrzewski, V. G.; Ortiz, J. V.; Foresman, J. B.; Ciolowski, J.; Stefanov, B. B.; Nanayakkara, A.; Challacombe, M.; Peng, C. Y.; Ayala, P. Y.; Chen, W.; Wong, M. W.; Andres, J. L.; Replogle, E. S.; Gomberts, R.; Martin, R. L.; Fox, D. J.; Binkley, J. S.; Defrees, D. J.; Baker, J.; Stewart, J. P.; Head- Gordon, M.; Gonzalez, C.; Pople, J. A. *Gaussian 94*, Revision A.1, Gaussian, Inc., Pittsburgh, PA, 1995.
(14) Froment, F.; Castella-Ventura, M.; Corset, J. Manuscript in preparation.
(15) Bauer, W.; Seebach, D. *Helv. Chim. Acta* **1984**, *67*, 1972.
(16) Kaufman, M. J.; Gronert, S.; Bors, D. A.; Streitwieser, A. *J. Am. Chem. Soc.* **1987**, *109*, 602.

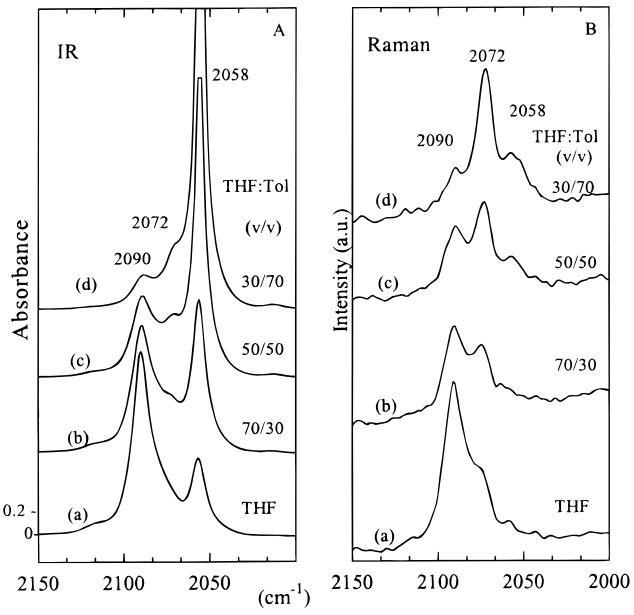

Figure 2. IR and Raman spectra in the ν(C≡N) region of **1** in THF−toluene solvent mixtures (C = 0.25 M).

at −108 °C, and with Streitwieser pK_a measurements.[16]

The IR and Raman spectra in THF−toluene mixtures (Figure 2A,B) are similar to those observed in THF−hexane at C = 0.25 M. In THF (Figure 2A, a; 2B, a), both IR and Raman spectra exhibit an intense band at 2090 cm^{-1} assigned to the monomeric ion pair **2**, its intensity decreasing regularly with the increasing proportion of toluene (Figure 2A, b−d). The Raman spectrum (Figure 2B, a) also shows a band at 2072 cm^{-1} and a smaller one at 2058 cm^{-1}, their intensity increasing regularly with the proportion of toluene (Figure 2B, b−d). The behavior of the IR spectra (Figure 2A) is more complicated, as the intensity of the band at 2058 cm^{-1} increases regularly with the amount of toluene, while that of the small shoulder at 2072 cm^{-1} remains almost constant.

The complex behavior of the intensity of the IR and Raman bands with the THF−hexane[3] and THF−toluene solvent composition led us to deconvolute the spectra of **1** (C = 0.25 M) into three Lorentzian components in these solvent mixtures. As an example, the integrated intensity of each ν(C≡N) band was plotted against the hexane molar fraction x in THF (Figure 3A,B). The band positions decrease only very slightly when the solvent polarity is reduced. As shown in Figure 3A, the IR integrated intensity of the 2090 cm^{-1} band decreases linearly with x, while that of the 2058 cm^{-1} band increases linearly with x, at the expense of the former. In contrast, the integrated intensity of the small band at 2072 cm^{-1} does not seem to vary with x; this may be explained by the superposition of two components varying in an opposite direction with x: (1) for the band of the solvent separated ion pair or of the free anion at 2094 cm^{-1} (Figure 1A), we underlined that the shoulder at 2075 cm^{-1} corresponds to a Fermi resonance with a skeleton mode combination (see above). Such a Fermi resonance may also exist for the monomeric ion pair band at 2090 cm^{-1}. This should explain the large asymmetry in the foot of the 2090 cm^{-1} band observed in THF (Figure 2A, a). The intensity of this Fermi component around 2075 cm^{-1} decreases proportionally to the monomeric ion pair concentration; (2) the small IR component at 2072 cm^{-1}, characterized in THF−toluene 30/70 v/v (Figure 2A, d) increases slowly from THF (Figure 2A, a) to THF−toluene solutions (Figure 2A, b−d); the same observation holds for THF−hexane media.

Scheme 1

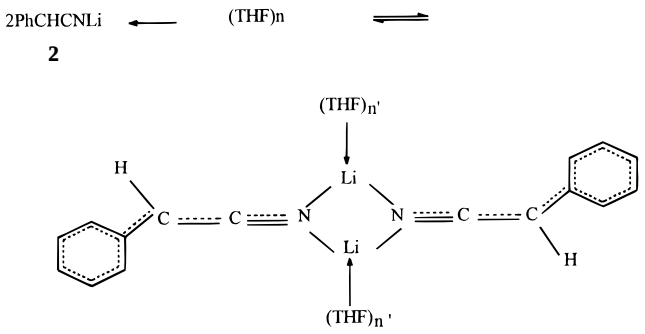

4

The evolution of the IR-integrated intensity of the monomeric species (ν(C≡N) band at 2090 cm^{-1}) was used to normalize the Raman spectra obtained for the different THF−hexane solvent mixtures (Figure 3B), since the spectral intensity depends on the experimental conditions, which may vary from sample to sample (laser power, sample position, etc.). The Raman-integrated intensity of the 2090 cm^{-1} band decreases with x, while those of the 2072 and 2058 cm^{-1} bands (Figure 3B) increase linearly with x, although the precision of this last one is lower, due to a small signal-to-noise ratio.

Thus, in contrast to our previous assumptions,[2] this detailed IR and Raman study clearly shows the existence of an equilibrium between only two species: a monomeric ion pair **2** and a dimeric ion pair **4** (Scheme 1).

The concentrations C_m and C_d of the monomeric ion pair **2** and dimeric ion pair **4** are, respectively, related to the concentration C of **1** (eq 1). Indeed, as the concentration C_m decreases linearly with the hexane molar fraction x in THF (eq 2, a and b are constants), the concentration C_d increases linearly with x (eq 3) (Figure 3A,B).

$$C = C_m + 2C_d \quad (1)$$

$$C_m = ax + b \quad (2)$$

$$C_d = -ax/2 + (C - b)/2 \quad (3)$$

This behavior is directly related to the decrease of the dielectric constant of the medium with x. The equilibrium constant between the monomeric and the dimeric species thus varies strongly with x.

The THF solvated dimer **4** in solution is not exactly centrosymmetric as usually observed for such dimers.[17] If the dimer **4** would be centrosymmetric, only one band should be seen: the antisymmetric ν_a (C≡N) in IR and the symmetric ν_s (C≡N) in Raman. Actually, the intensity exclusion rule is not observed: the pseudomodes ν_a (C≡N) at 2058 cm^{-1} and ν_s (C≡N) at 2072 cm^{-1} are both active in Raman and IR.

To ascertain the predominance of the equilibrium, represented in Scheme 1, over the other possible equilibria (free ions, trimeric or tetrameric species, etc.) in

(17) Chabanel, M. *Pure Appl. Chem.* **1990**, *62*, 35.

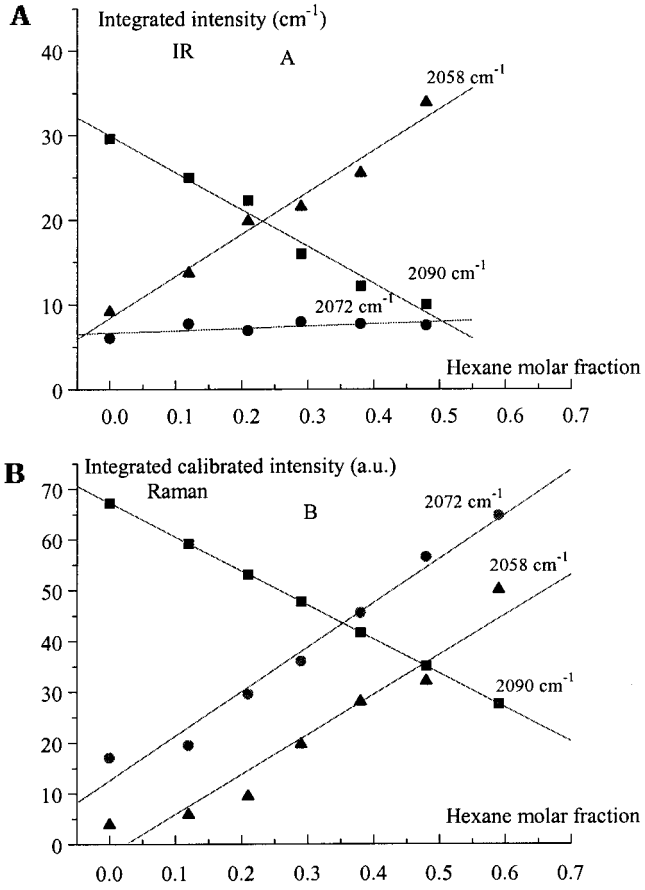

Figure 3. Variation of the integrated intensity of each ν(C≡N) band in function of the hexane molar fraction x in THF: A in IR; B in Raman (C = 0.25 M).

THF, THF−hexane, and THF−toluene solvent mixtures and to estimate the concentration of the monomer C_m and of the dimer C_d, we have used the method proposed by Chabanel and Paoli[18] in the case of the dimerization of LiSCN.

The integrated intensity of the bands at 2090 cm^{-1} A_m and 2058 cm^{-1} A_d for the monomeric and the dimeric species is, respectively

$$A_m = \epsilon_m l C_m \quad (4)$$

$$A_d = \epsilon_d l C_d \quad (5)$$

where l is the cell thickness and ϵ_m and ϵ_d are the integrated molar absorption coefficients of these species.

From eqs 1, 4, and 5 it becomes

$$\frac{A_d}{lC} = -\frac{A_m}{lC}\frac{\epsilon_d}{2\epsilon_m} + \frac{\epsilon_d}{2} \quad (6)$$

As we used solvent mixtures covering a very short range of dielectric constant values, from 7.58 in THF to 4.24 in the THF−toluene 30/70 v/v medium, we may assume that the integrated molar absorption coefficients ϵ_d and ϵ_m remain constant. In Figure 4 are presented the variations of A_d/lC as a function of A_m/lC for THF, THF−hexane, and THF−toluene media (some solutions have been prepared and measured two times to check the accuracy of the measurements). It may be observed

(18) Chabanel, M.; Paoli, D. *J. Chim. Phys.* **1980**, 77, *10*, 913.

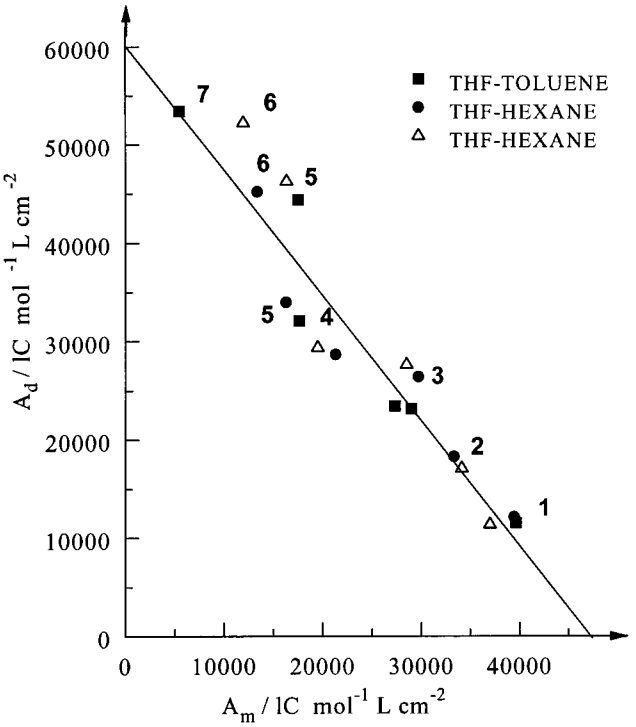

Figure 4. Diagram for the determination of the integrated molar absorption coefficients of the monomer **2** and of the dimer **4** (C = 0.25 M). Percent v/v of hexane or toluene in the THF solvent mixtures for the points 1−7: 1, 0; 2, 18; 3, 30; 4, 40; 5, 50; 6, 60; 7, 70. A_d/lC and A_m/lC are expressed in mol^{-1} L cm^{-2}.

Table 1. Comparison of the Integrated Molar Absorption Coefficient ϵ^a of the ν(C≡N) Bands of Lithium Thiocyanate, Lithiated Phenylacetonitrile Monomeric and Dimeric Species, and Phenylacetonitrile Free Anion

solvent	THF, THF−toluene, THF−hexane	BuOAc[c]
dielectric constant	7.58−4.24	5.01
salt	PhCHCNLi	LiSCN
$-\epsilon_m$	47 500	24 900
$-\epsilon_d$	121 800	59 100
$-\epsilon_f$[b]	46 000	

[a] The units are mol^{-1} L cm^{-2}. [b] Measured integrated molar absorption coefficient ϵ_f for the free anion in (35/65, v/v) THF−HMPA (dielectric constant: 17.20). [c] Reference 18.

that all these points (1−7) are close to a straight line corresponding to eq 6. It must be taken into account that the measurements performed with a 0.003 cm cell are less precise, due to the large intensity of the band at 2058 cm^{-1} in low dielectric constant media (points 4−7). The integrated molar absorption coefficients ϵ_d and ϵ_m were determined from the intersections of this straight line with the axis. These values are reported in Table 1 and compared to those measured for the free anion band at 2094 cm^{-1} ϵ_f in THF−HMPA 35/65 v/v solvent mixture (dielectric constant = 17.20) and for LiSCN in *n*-butyl acetate (dielectric constant = 5.01, near those of THF, THF−hexane, or THF−toluene media). The close values ϵ_d/ϵ_m of 2.4 for LiSCN and 2.6 for PhCHCNLi confirm that these two dimeric species exhibit a similar structure. These values seem also to indicate that the C_1-N bond polarity is greater in the dimeric species compared to the monomeric ones. Finally, the ϵ_f value found for the phenylacetonitrile free anion in THF−HMPA is as expected of the same order of magnitude as ϵ_m of the

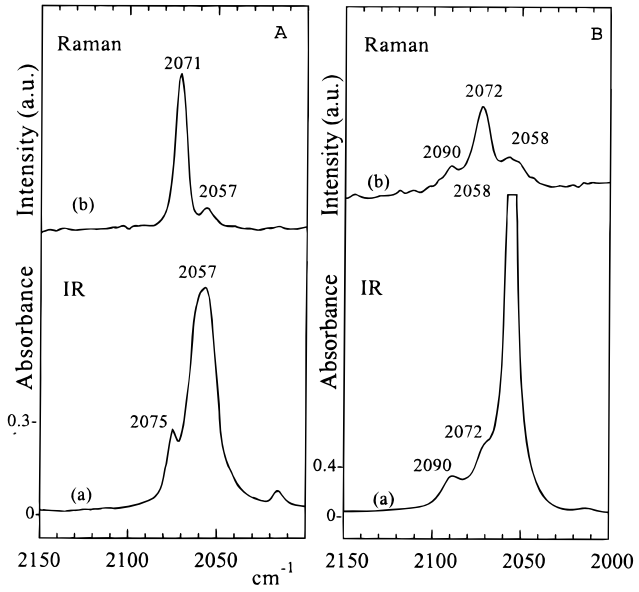

Figure 5. IR and Raman spectra in the ν(C≡N) region (A) of the TMEDA-solvated solid-state dimer **3** and (B) of the THF-solvated dimer **4** in THF−toluene 30/70 v/v (C = 0.25 M).

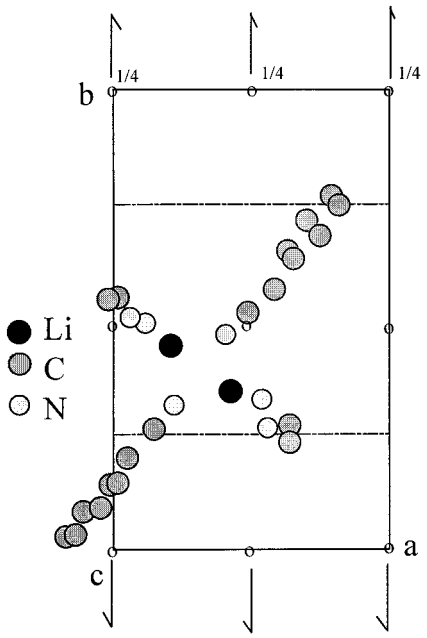

Figure 6. Projection of one dimer on the (a,b) plane of the unit cell $P2_1/n$ of the TMEDA-solvated solid-state dimer **3**. (helicoidal axis ⌐; glide plane —·—; inversion center ○). See also ref 7b, Figure 14.

monomeric ion pair **2**, thus showing the consistency of the measurements and assignments.

(2) Structure of the THF-Solvated Dimer 4. Comparison with the crystalline TMEDA-Solvated Dimer 3, Described by Boche. To determine the dimer structure in solution, we have compared our IR and Raman spectra of **4** with those of the TMEDA-solvated dimer **3** in the solid state that we have prepared and that was previously analyzed by X-ray crystallography.[7] The IR spectrum of **3** (Figure 5A, a) is slightly different from that reported by Boche;[7] the latter exhibits only a broad component at 2065 cm^{-1}, while the former shows two bands at 2075 and 2057 cm^{-1}. The 2075 cm^{-1} one, overlapped by the foot of the intense band at 2057 cm^{-1}, is thus seen at a slightly higher frequency than the intense ν_s (C≡N) band observed at 2071 cm^{-1} in the Raman spectrum (Figure 5A, b). The ν_a (C≡N) IR and Raman components at 2057 cm^{-1} lie as expected at the same wavenumber. Compound **3** crystallizes in the monoclinic system $P2_1/n$ with four dimers per unit cell; these dimers correspond to each other by an inversion center and a helicoidal axis parallel to b. They are not located on an inversion center site of the unit cell as is usually observed for centrosymmetric dimers.[19] The difference between this species and a centrosymmetric one is clearly seen in Figure 6, where the projection on the (a,b) plane of only one dimer in the unit cell is shown. Although the two anion planes are close to a projection plane containing the c axis, they are located at an angle of 95.7° and 103.5°, respectively, to the least-squares plane of the Li_2N_2 ring.

The comparison between the IR and Raman spectra of the THF-solvated dimer **4** in solution (Figure 5B, a, b), with those of **3** in the solid state (Figure 5A, a, b) shows only a very small frequency shift of the order of 1 cm^{-1}, but the frequency difference ν_s(C≡N) − ν_a(C≡N) equal to 14 cm^{-1} remains the same. To calculate the coupling force constant between the two C≡N vibrators of the dimer from its solid-state geometry, we have assumed a pure dipolar coupling between these two vibrators. The dipoles are located at the center of the C≡N bonds,[20] and the polarity of the C≡N bond in the dimer is taken equal to that measured for the free anion in THF−HMPA (Figure 1 and Table 1). This calculation leads to a frequency difference ν_s(C≡N) − ν_a(C≡N) equal to 22 cm^{-1}, which is of a good order of magnitude compared to the observed one equal to 14 cm^{-1}.

Finally, the identity of the coupling ν_s(C≡N) − ν_a(C≡N), the small frequency shift observed between the solid-state TMEDA-solvated dimer **3** and the THF-solvated dimer **4** solution, and the activity of both modes ν_a(C≡N) and ν_s(C≡N) in IR and Raman confirm that the dimer **4** is not centrosymmetric and has a structure close to that of **3**, the two phenyl groups lying in an anti arrangement. Furthermore, this noncentrosymmetry of the dimer structure **3** is not due to the packing forces in the solid state but is related to the deviation to coplanarity of the two anionic moieties.

(3) Structure of the Monomeric Ion Pair 2. In our previous work,[2] we assigned to the lithiated monomeric species **2** a linear tight ion pair structure according to the ^{13}C NMR data. This assignment ought to be revised, as Collum[6] did not observe either a $^1J(^{15}N-^6Li)$ coupling in 2/1 THF−pentane or 2/1 THF−toluene solvent mixtures or a $^1J(^{13}C-^6Li)$ coupling in toluene-d_8−THF-d_8 mixtures, at low temperature. Thus, the monomeric tight ion pair structure could not be confirmed at low concentration and temperature in THF. Two possibilities were envisioned to explain this phenomenon: a rapid intramolecular $C_{2'}$Li and NLi chemical exchange in THF or the existence of a solvent-separated ion pair. To elucidate

(19) (a) *International Tables for X-ray Crystallography*; Henry, N. F. M., Lonsdale, K., Eds.; Kynoch Press: Birmingham, 1965; Vol. 1. (b) Vogel-Weil, C.; Corset, J. *Spectrochim. Acta* **1995**, *A51*, 2357.

(20) Baron, M. H.; Jaeschke, H.; Moravie, R. M.; De Loze, C.; Corset, J. Metal−Ligand Interactions. In *Organics Chemistry and Biochemistry*; Pullman B., Goldblum N., Eds; Ridel D. Publishing Co.: Dordrecht, Holland, 1977; Part 1, p 171.

Table 2. Optimized Structures and Total Energies Calculated for the CH_3CN[a] and $PhCH_2CN$ Molecules and Their Derived Free Anions and Lithiated Ion Pairs, with the 3-21+G* Basis Set at the HF Level

geometrical parameters[a]		molecule		free anion		linear monomeric ion pair		bridged monomeric ion pair	
b	*c*	CH_3CN	$PhCH_2CN$	CH_2CN^-	$PhCHCN^-$	CH_2CNLi	PhCHCNLi	CH_2CNLi	PhCHCNLi
C_1N	$C_{1'}N$	1.134	1.134	1.159	1.152	1.176	1.170	1.159	1.153
C_2C_1	$C_{2'}C_{1'}$	1.460	1.468	1.385	1.391	1.332	1.342	1.394	1.391
	$C_{2'}C_{3'}$		1.518		1.416		1.453		1.446
C_2C_1N	$C_{2'}C_{1'}N$	180.0	179.3	178.3	179.2	180.0	179.7	161.9	167.9
τNC_1C_2H	$\tau NC_{1'}C_{2'}C_{3'}$	0.0	179.7	105.7	180.0	0.0	180.2	111.9	55.5
	$\tau C_{1'}C_{2'}C_{3'}C_{8'}$		−89.6		180.0		180.0		183.6
	$\tau C_{1'}C_{2'}C_{3'}C_{4'}$		89.7		0.0		0.0		−3.2
C_1C_2H	$C_{1'}C_{2'}H$	109.7	107.8	117.6	116.9	120.0	116.9	115.0	119.5
	$C_{1'}C_{2'}C_{3'}$		112.1		123.6		123.7		118.7
Σ angles C_2[d]	Σ angles $C_{2'}$[d]			352.3	360.0	360.0	360.0	344.4	359.2
LiN	LiN					1.763	1.773	2.161	2.524
LiC_1	$LiC_{1'}$					2.939	2.943	1.984	2.127
LiC_2	$LiC_{2'}$					4.271	4.284	2.207	2.148
	$LiC_{3'}$						5.234		2.285
	$LiC_{4'}$						5.186		2.398
LiC_1C_2	$LiC_{1'}C_{2'}$					180.0	179.9	79.5	71.8
	$LiC_{2'}C_{3'}$						123.8		76.2
τLiC_1C_2H	$\tau LiC_{1'}C_{2'}C_{3'}$					0.0	180.7	111.9	60.9
	$\tau LiC_{2'}C_{3'}C_{4'}$						0.0		54.6
	$\tau LiC_{2'}C_{3'}C_{8'}$						180.0		−118.6
	$C_{3'}C_{4'}$		1.387		1.420		1.402		1.409
	$C_{3'}C_{8'}$		1.387		1.420		1.401		1.415
	$C_{4'}C_{5'}$		1.385		1.377		1.382		1.397
	$C_{8'}C_{7'}$		1.385		1.377		1.381		1.371
	$C_{5'}C_{6'}$		1.385		1.392		1.386		1.374
	$C_{7'}C_{6'}$		1.385		1.392		1.387		1.399
total energies[e]		−131.276 86	−359.665 43	−130.662 48	−359.085 60	−138.089 99	−366.491 33	−138.093 62 (−2.28)	−366.491 96 (−0.40)

[a] The units are Å for bond lengths and deg for angles. The carbanion coordinates for all these structures are given as Supporting Information. [b] Geometrical parameters corresponding to the acetonitrile derivatives. [c] Geometrical parameters corresponding to the phenylacetonitrile derivatives. [d] Σ angles $C_2 = C_1C_2H + HC_2H + C_1C_2H$; Σ angles $C_{2'} = C_{1'}C_{2'}C_{3'} + C_{3'}C_{2'}H + C_{1'}C_{2'}H$. [e] The units are H (hartree) for total energies and kcal/mol for differences of energy between the bridged and linear ion pairs (given in parentheses).

Table 3. Comparison of Selected IR, Raman, ^{13}C NMR, X-ray, and ab Initio Calculation Data for Phenylacetonitrile Free Anion and Lithiated Ion pairs

	free anion THF−HMPA (50/50 v/v)	monomeric linear 12-crown-4 solvated Li ion pair[a]	monomeric THF solvated Li ion pair **2**		dimeric THF−toluene (30/70 v/v) solvated Li ion pair **4**	dimeric TMEDA solvated Li ion pair **3**	
			linear	bridged			
νCN (cm^{-1}) IR	2094	2089 (THF)		2090	2065 (2058)	2064	(2057)[b]
νCN (cm^{-1}) Raman	2094			2090	(2072)		(2071)[b]
$\Delta\delta^{13}C_{1'}$ [c]	+16.3	+22.5		+25.1	+32.3		
$\Delta\delta^{13}C_{2'}$	+11.9	+10.2		+8.8	+9.1		
$\Delta\delta^{13}C_{3'}$	+20.9	+20.6		+18.6	+17.0		
$\Delta\delta^{13}C_{6'}$	−20.5	−16.2		−16.3	−13.5		
$^1J(^{13}C_{2'}H)$ (Hz)	161			163.1	163.6		
LiN[g]		1.950	1.773[d]	2.524[d]		2.035[f]	2.024[e] 2.012[e]
$C_{1'}N$	1.152[d]	1.168	1.170[d]	1.153[d]		1.212[f]	1.171[e]
$C_{1'}C_{2'}$	1.391[d]	1.383	1.342[d]	1.391[d]		1.342[f]	1.372[e]
$C_{2'}C_{3'}$	1.416[d]	1.430	1.453[d]	1.446[d]		1.437[f]	1.442[e]
$C_{1'}C_{2'}C_{3'}$	123.6[d]	123.6	123.7[d]	118.7[d]		123.9[f]	124.5[e]
Σ angles $C_{2'}$[h]	360.0[d]	360.0	360.0[d]	359.2[d]		360.0[f]	360.0[e]

[a] Reference 7d. [b] Figure 5A. [c] Variations $\Delta\delta$ (δ in anion − δ in $PhCH_2CN$) in ppm relative to TMS refs 2 and 7d. [d] Calculated values with the 3-21+G* basis set at the HF level (Table 2). [e] X-ray data from ref 7c. [f] PM3-calculated values from ref 8. [g] Bond lengths are given in Å and angles in deg. [h] Σ angles $C_{2'} = C_{1'}C_{2'}C_{3'} + C_{3'}C_{2'}H + C_{1'}C_{2'}H$.

the location of the lithium cation in the monomeric species **2**, we have calculated by ab initio methods using the 3-21+G* basis set the following structures: the neutral species $PhCH_2CN$, the free anion $PhCHCN^-$, and the monomeric ion pair PhCHCNLi (**2**). Similar ab initio calculations have already been achieved with different basis sets (STO-3G,[21] 3-21G, 6-31G*, and 6-31+G*[9]) for acetonitrile (CH_3CN) and its carbanionic derivatives and with the STO-3G[22] and 3-21G[5] basis sets for the free ion $PhCHCN^-$.

Our results for CH_3CN and $PhCH_2CN$ and their carbanionic species are given in Table 2 and Figure 7. The geometrical parameters of CH_3CN derivatives are very close to those calculated in former theoretical studies.[9,21] It is interesting to notice that for $PhCH_2CN$ (Figure 7, a′), the plane containing the N, $C_{1'}$, $C_{2'}$, and $C_{3'}$

(21) Moffat, J. B. *J. Chem. Soc., Chem. Commun.* **1980**, 1108.
(22) Loupy, A.; Lefour, J. M.; Deschamps, B.; Seyden-Penne, J. *Nouv. J. Chim.* **1980**, *4*, 121.

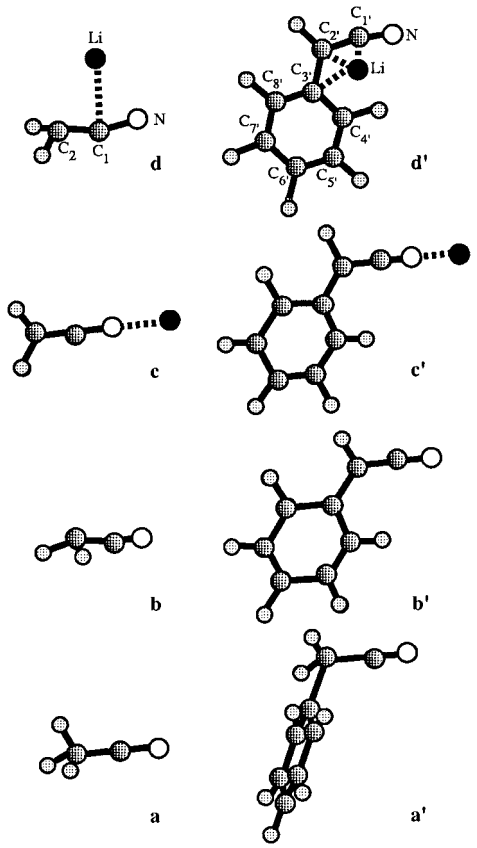

Figure 7. Comparison of the stable structures calculated for the CH_3CN and $PhCH_2CN$ molecules (a,a′), their derived free anion (b,b′), their linear-lithiated monomeric ion pair (c,c′), and their bridged lithium monomeric ion pair (d,d′). The structures are calculated with the 3-21+G* basis set at the HF level. The Cartesian coordinates of these optimized structures are given as Supporting Information.

atoms is perpendicular to that of the phenyl ring. The $C_{2'}C_{1'}$ and $C_{1'}N$ bond lengths are very similar to those of CH_3CN.

In the free-anion species $PhCHCN^-$ (Figure 7, b′, Table 2), the cyano group becomes coplanar with the phenyl ring due to a partial conjugation, the $C_{2'}$ carbon hybridization being sp^2 ($C_{1'}C_{2'}H + C_{3'}C_{2'}H + C_{1'}C_{2'}C_{3'} = 360.0°$); the $C_{1'}N$ and $C_{2'}C_{1'}$ bond lengths are analogous to those observed in CH_2CN^-, indicating that the charge delocalization takes place mainly into the phenyl ring,[23] as shown by the shortening of the $C_{2'}C_{3'}$ bond. These calculations are in agreement with the IR frequency shifts, $\Delta\delta^{13}$C NMR chemical shifts ($\delta_{neutral} - \delta_{anion}$), and the large $^1J(C_{2'}-H)$ coupling constant value [2,14] (Table 3).

On the other hand, in the case of the monomeric ion pair, the energy difference between the structure involving a lithium-bridged arrangement (Figure 7, d and d′) and the one exhibiting a linear C≡N···Li geometry (Figure 7, c and c′, Table 2) depends on the basis set used. With the 3-21G basis set, the linear CH_2CN monomeric ion pair is more stable than the bridged one by +4.8 kcal/mol,[9] whereas the bridged monomer is stabilized with respect to the linear one by −2.28 and −5.84 kcal/mol with the 3-21+G* and 6-31G*[9] basis sets, respectively; when the HF total energies obtained with the 6-31G* basis set are corrected for electron correlation via the second-order Møller−Plesset perturbation method (MP2), the energy shift decreases to −9.7 kcal/mol[9] (the MP2 energies have been calculated for the equilibrium structures already optimized at the HF level). We found two similar stable geometries for the PhCHCNLi monomeric ion pair **2** (Figure 7, d′ and c′). In the same way, the linear structure c′ is more stable by +5.63 kcal/mol with the 3-21G basis set, whereas the bridged structure is lower in energy by −0.40 kcal/mol with the 3-21+G* basis set.

When solvation by water is taken into account through MNDO calculations,[9] the relative stabilities of solvated acetonitrile ion pair c and d (Figure 7) remain unchanged, as the total solvation energies of the two species are nearly the same. Assuming that the bridged monomeric form is solvated by two water molecules and the linear one by three water molecules, and using the MNDO calculated solvation energies determined by Schleyer,[9] the bridged form remains the more stable by 1.1 kcal/mol. However, Enders[23] has shown by ab initio calculations that water reacts with the more stable lithiated acetonitrile bridged species. To overcome this problem, he made the hypothesis that solvation energies calculated for the linear species are the same for the bridged one, as roughly found by MNDO. The much higher solvation energies thus found by MP2/6-31G*//RHF/6-31G* ("//" means at the geometry of) lead to a linear ion pair more stable than the bridged one by 6.4 kcal/mol.

Our spectroscopic studies concerning the dimeric species show that the solvation of **3** and **4** by two different donor molecules such as TMEDA and THF, respectively, does not appreciably influence the structure of the dimer. MNDO calculations have shown that for the CH_2CNLi dimer the solvation by water changed considerably the dimer structure.[9]

At the present time, it is difficult to estimate, at a reasonable cost, the solvation of such carbanions by THF, since water cannot be used as a realistic model for THF. Experimental arguments are thus necessary to support one structure rather than the other.

We have summarized in Table 3 the calculated and observed X-ray structure data, the measured IR and Raman ν (C≡N) band wavenumbers, and $\Delta\delta^{13}$C NMR chemical shifts for the following species: free anion, solid 12-crown-4 Li-solvated linear monomeric ion pair,[7d] THF-solvated linear and bridged monomeric ion pairs **2**, THF-solvated dimer **4**, and solid TMEDA-solvated dimer **3**. We notice that the structure of the linear monomeric ion pair **2**, calculated by ab initio methods with the 3-21+G* basis set at the HF level, is in excellent agreement with the X-ray data of the 12-crown-4 Li-solvated ion pair.[7d] The $C_{1'}N$ bond length for the latter is a little smaller than that of the linear ion pair **2**, while the other geometry parameters remain very similar. Consequently, the ν(C≡N) wavenumber of the linear ion pair should be smaller than the measured one for the crown Li-solvated ion pair at 2089 cm^{-1}, i.e., close to the mean wavenumber of the dimer **3** at 2064 cm^{-1}. The $C_{1'}N$ bond length observed in the dimer is indeed similar to that calculated for the linear ion pair. The expected wavenumber lowering of the linear ion pair is also in agreement with that observed in THF for the PhCHCNK aggregated ion pairs at 2070 cm^{-1},[2] the K^+ cation being less polarizing than the Li^+ one.

(23) Raabe, G.; Zobel, E.; Fleischhauer, J.; Gerdes, P.; Mannes, D.; Müller, E.; Enders, D. *Z. Naturforsch.* **1991**, *46a*, 275.

The 2090 cm^{-1} wavenumber of the ν(C≡N) mode observed for the monomeric lithiated ion pair in THF is thus in favor of the bridged ion pair structure in which the Li^+ cation does not interact with the nitrogen atom of the C≡N group. The comparison of the calculated $C_{1'}N$ bond length of the bridged structure (1.153 Å) with that of the free anion (1.152 Å) shows that their ν(C≡N) wavenumbers are of the same order of magnitude. The Li···N≡C interaction is responsible for the $C_{1'}N$ bond lengthening in the linear crown Li-solvated ion pair, the linear ion pair **2**, and the dimer **3** (Table 3). The charge delocalization toward the phenyl ring also contributes strongly to the polarization of the phenyl ring bonds as already noticed[2] and to the $C_{6'}$ shielding leading to $\Delta\delta^{13}C_{6'}$ values of − 20.5, −16.2, and −13.5 ppm for the free anion, the crown Li-solvated ion pair, and the dimer, respectively. In the lithiated bridged ion pair, this conjugation is weakened and the $C_{2'}$ carbon charge is strengthened. We correlatively observed an upfield shift[2] of the $\delta^{13}C_{2'}$ (31.9 ppm) of the bridged form relative to those of the free anion (35.05 ppm) and monomeric linear 12-crown-4 lithiated ion pair (33.4 ppm). A similar effect has been reported for the lithium ester enolate of methyl isobutyrate.[24] Furthermore, in the bridged form the lithium cation interactions with $C_{2'}$, $C_{3'}$, and $C_{4'}$ carbons strongly polarize the phenyl ring, inducing a $\Delta\delta^{13}C_{6'}$ shielding of −16.3 ppm similar to that of the linear crown ion pair (Table 3). These interactions of the lithium with the phenyl ring have been evidenced by a variable low-temperature ^{13}C NMR study of the free anion in THF−HMPA 50/50 v/v solvent mixture and of the monomeric ion pair **2** in THF. The temperature lowering of the free anion solution in THF−HMPA induces the splitting of the $C_{5'}$, $C_{7'}$ and of the $C_{4'}$, $C_{8'}$ carbon signals, respectively, at +10 and −10 °C on a 250 MHz spectrometer for C = 0.25 M. Using the approximate expression established by Gutowsky and Holm[25] to obtain the chemical exchange rate K at the coalescence temperature T_c, we calculated from the Eyring equation[26] the free enthalpy of activation $\Delta G^{\ddagger}$ at the coalescence temperature, that is to say the rotation barrier of the phenyl group, if the entropy change between the two conformers is negligible. We thus obtain $\Delta G^{\ddagger}$ values of 56.9 and 59.6 J mol^{-1} from the $C_{4'}$,$C_{8'}$ and the $C_{5'}$,$C_{7'}$ splittings, respectively. The close values obtained for $\Delta G^{\ddagger}$ indicate that these splittings are due to the two conformers related to the different substituents H and C≡N on the $C_{2'}$ carbon. This barrier value is of a good order of magnitude for a rotation around a partial $C_{2'}C_{3'}$ double bond; actually, a value of 71 J mol^{-1} for the diethyl [(carbomethoxy)methyl] phosphonate free anion[27] and of 48.9 J mol^{-1} for the potassium diphenylmethyl anion in DMSO[28] have been reported.

For the monomeric bridged ion pair **2** in THF, only a splitting of the signals corresponding to $C_{4'}$ and $C_{8'}$ was observed at −60 °C on a 400 MHz spectrometer for C = 0.25 M leading to a smaller $\Delta G^{\ddagger}$ value of 44.8 J mol^{-1}. This lower rotation barrier of the phenyl group is in good agreement with the lengthening of the $C_{2'}C_{3'}$ bond when going from the free anion to the bridged ion pair (Table 2). Furthermore, the splitting of 67.2 Hz seen on a 400 MHz spectrometer, which corresponds to a splitting of 42 Hz on a 250 MHz spectrometer, is much larger than those seen in the free anion $\delta C_{4'}-\delta C_{8'} = 12$ Hz and $\delta C_{5'}-\delta C_{7'} = 26$ Hz. This strong splitting observed only on the $C_{4'}$,$C_{8'}$ signals may be correlated with the short $LiC_{4'}$ bond length of 2.398 Å (Table 2) in the bridged form. The charge polarization on the three carbon atoms $C_{2'}$, $C_{3'}$, and $C_{4'}$ thus induces an asymmetry in the phenyl ring, the $C_{4'}C_{5'}$ bond length being 0.026 Å longer than the $C_{8'}C_{7'}$ one (Table 2).

In the bridged monomeric ion pair, the $LiC_{2'}$ bond length of 2.148 Å (Table 2) is a little shorter than the LiC_{α} bond length of the benzyllithium triethylenediamine[29] derivative, which is equal to 2.21 Å as shown by X-ray analysis. Recently, Fraenkel[30] has reported low $^1J(^{13}C-^6Li)$ values of 3−4 Hz for several benzylic lithium ion pairs in THF. These values were observed under special conditions: in a very dilute solution (0.005 M) of benzyllithium that is ^{13}C enriched at C_{α} or in the presence of a stabilizing ligand. As these conditions were not fulfilled, it may be one of the reasons why such $^1J(^{13}C_{2'}-^6Li)$ coupling was not evidenced[6] for the lithium-bridged monomeric phenylacetonitrile. Moreover, the LiN distance (2.524 Å) is greater in the bridged monomeric ion pair than in the linear one (1.773 Å). This may also prevent the observation of $^1J(^{15}N-^6Li)$ coupling, independently of any exchange process in THF. As it is known that the $^1J(^{13}C_{2'}-H)$ coupling is both depending on the hybridization and on the charge of the carbon atom,[31] the high $^1J(C_{2'}-H)$ coupling constant value found (Table 3) for the bridged ion pair may be due to the charge localization on this carbon.

Conclusion

We have shown that in the case of the lithiated phenylacetonitrile **1** only two species are in equilibrium at room temperature in THF, THF−hexane, and THF−toluene solvent mixtures: a monomeric ion pair **2** and a dimeric one **4**. The equilibrium position was directly related to the dielectric constant of the medium, and the integrated molar absorption coefficients of each species was determined. Their values fit well with the monomer−dimer equilibrium in these media.

The comparison of IR, Raman, and ^{13}C NMR data with ab initio calculations confirmed the bridged structure of the lithiated monomeric ion pair **2**, the lithium cation interacting with the $C_{2'}$ carbon α to the nitrile moiety, the $C_{3'}$ ipso carbon, and the $C_{4'}$ carbon of the phenyl group. Variable low-temperature ^{13}C NMR evidenced both a lower rotational barrier of the phenyl group and a greater inequivalency of the ortho carbons for the monomeric ion pair **2** relative to the free anion.

Supporting Information Available: The atomic coordinates for all the optimized structures calculated at the HF level with the 3-21+G* basis set are given in tables with reference to the atom numbering of Figure 7 (4 pages). This material is contained in libraries on microfiche, immediately follows this article in the microfilm version of the journal, and can be ordered from the ACS; see any current masthead page for ordering information.

JO9614497

(24) Weiss, H.; Yakimansky, A. V.; Müller, A. H. E. *J. Am. Chem. Soc.* **1996**, *118*, 8897.
(25) Gutowsky, H. S.; Holm, C. H. *J. Chem. Phys.* **1956**, *25*, 1228.
(26) Glasstone, S.; Klaider, K. J; Eyring, H. *Theory of rate processes*; McGraw Hill: New York, 1941; p 185.
(27) Bottin-Strzalko, T.; Corset, J.; Froment, F.; Pouet, M. J.; Seyden-Penne, J.; Simonnin, M. P. *J. Org. Chem.* **1980**, *45*, 1270.
(28) Bank, S.; Dorr, R. *J. Org. Chem.* **1987**, *52*, 501.
(29) Patterman, S. P.; Karle, I. L.; Stucky, G. D. *J. Am. Chem. Soc.* **1970**, *92*, 1150.
(30) Fraenkel, G.; Martin, K. V. *J. Am. Chem. Soc.* **1995**, *117*, 10336.
(31) O'Brien D. H. in *Comprehensive Carbanion Chemistry*; Buncel, E., Durst, T., Eds.; Elsevier: Amsterdam, 1980; Part A, Chapter 6.